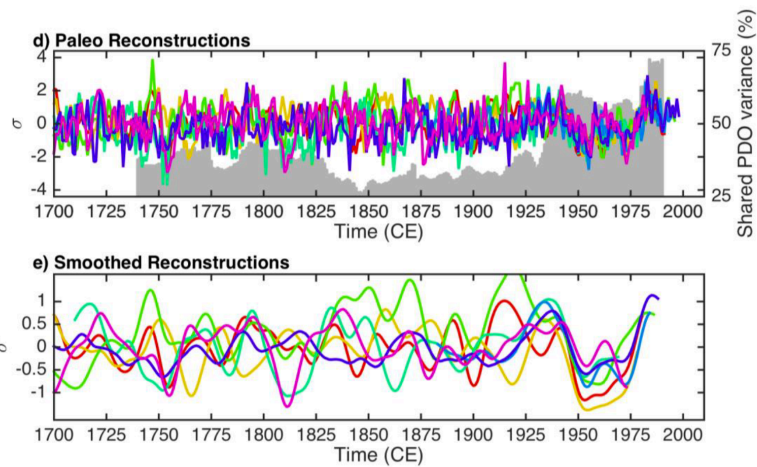
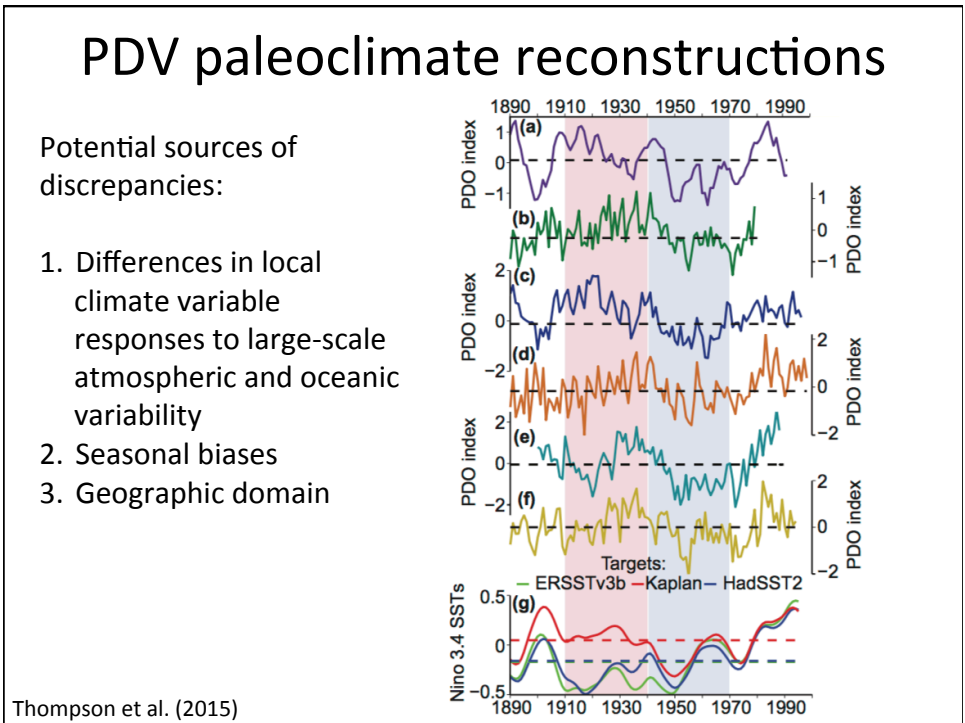
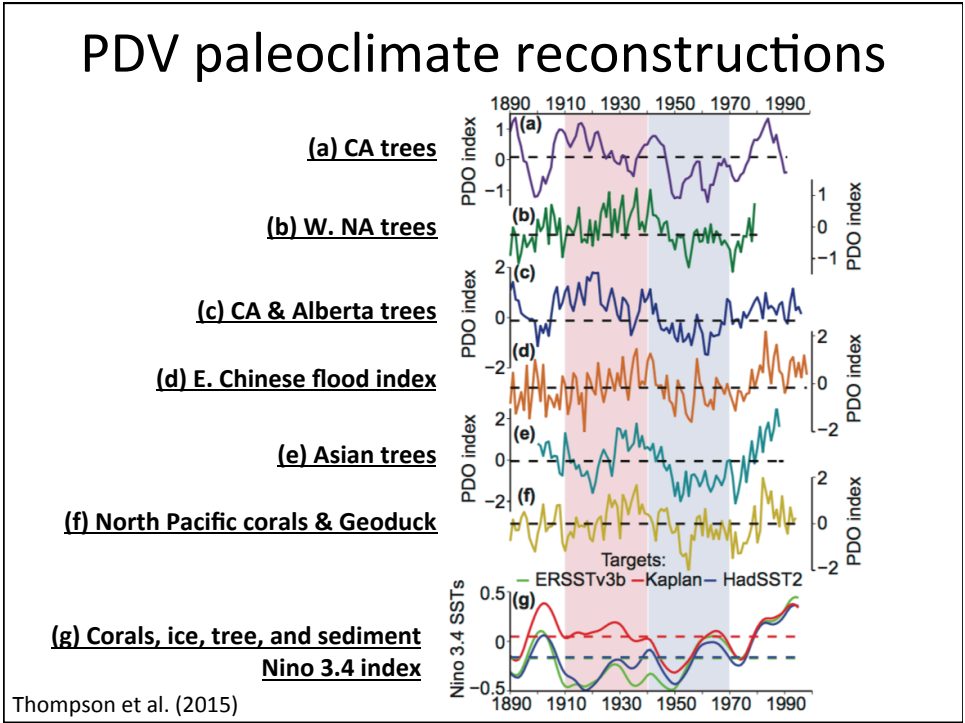


PDVII: Past & Future

PDV paleoclimate reconstructions



Newman et al. 2016



Recall: PDO and ENSO precip teleconnections

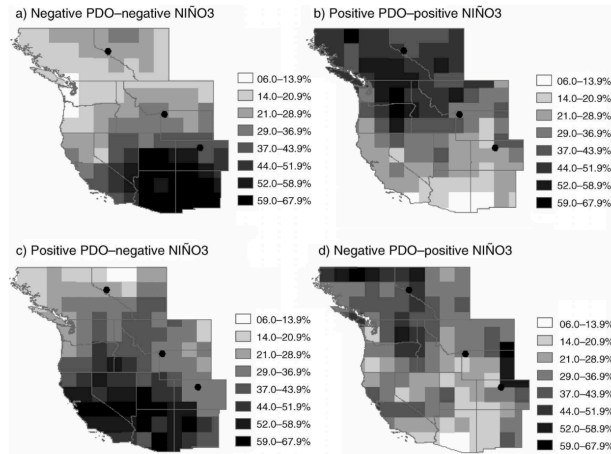
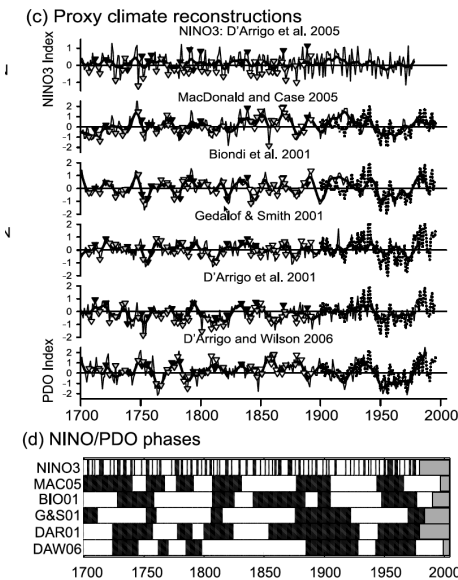


FIG. 7. Maps depicting the percentages of years classified as extreme drought (first-quartile PDSI) during the four categorical combinations of the PDO and ENSO phases across the western United States and Canada. The three study areas are represented by solid circles. Schoennagel et al (2005)

Paleo PDO: impact on fires?



Kipfmüller et al. 2012

Fire years vs PDO/ENSO

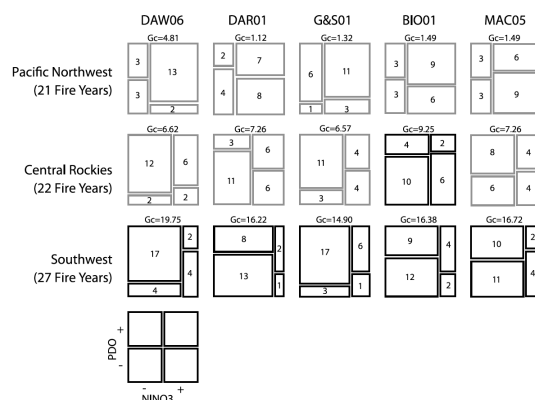


Figure 3. Mosaic plots of contingent relationships between widespread fire years and proxy estimates of the PDO and NINO3 for three regions across the western United States. The numbers in each box represent the observed number of fire events falling within each contingent class. William's-corrected G statistics are shown above each plot (critical value of $\chi^2_{(3,p=0.05)} = 7.815$). Significant G -test results are indicated by mosaic plots outlined in black.

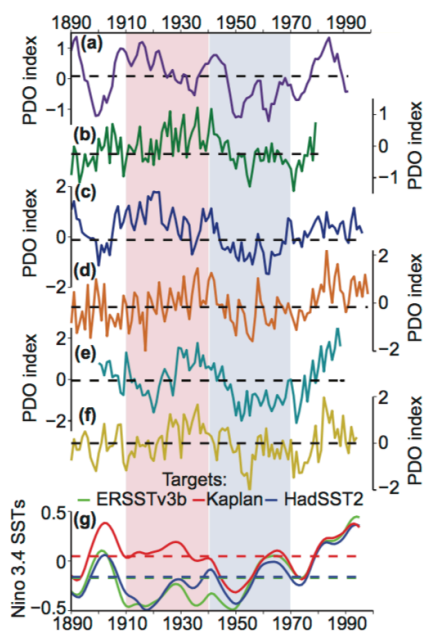
Kipfmüller et al. 2012

PDV paleoclimate reconstructions

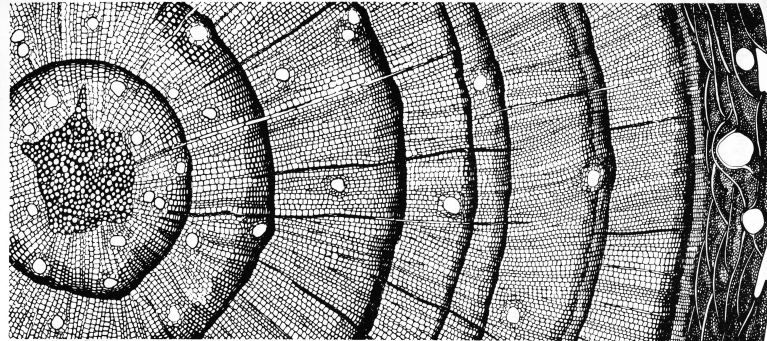
Potential sources of discrepancies:

1. Differences in local climate variable responses to large-scale atmospheric and oceanic variability
2. Seasonal biases
3. Geographic domain
4. Statistical removal of biological growth-related trends (trees)
5. etc

Thompson et al. (2015)

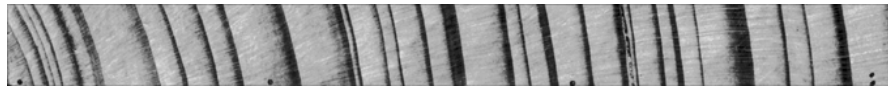


Tree ring processing for ontogenetic growth

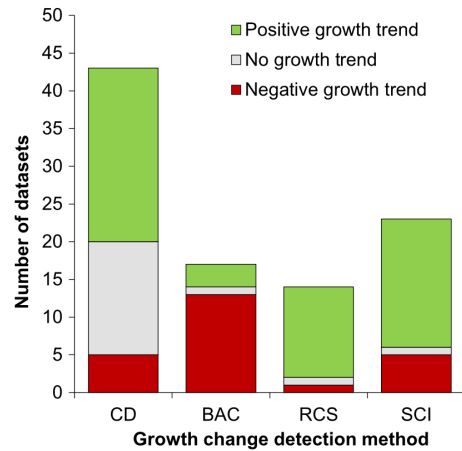
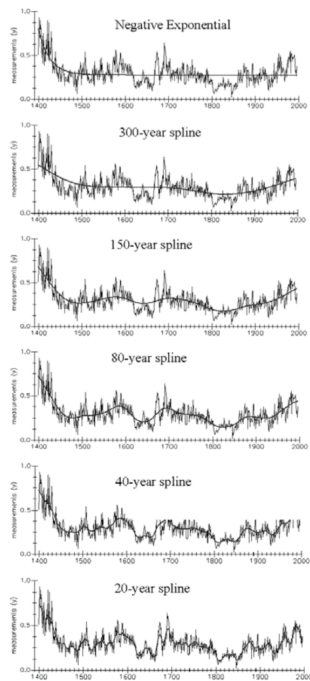


← Pith
(center of tree)

Bark →
(outside of tree)

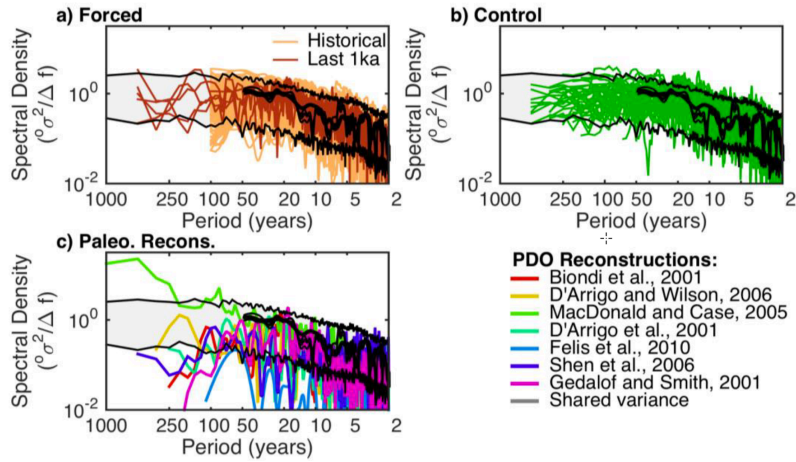


Removing ontogenetic (growth) effects



Peters et al. (2015)

PDO spectra, modeled vs paleo



Newman et al. 2016

Simulated PDO

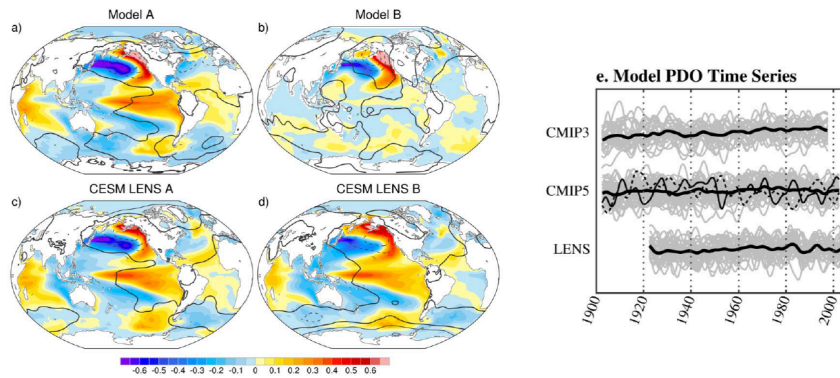


Figure 8. The PDO over the historical record as simulated by coupled CGCMs. (a and b) Same as Fig. 1a except showing two selected members of the “historical” CMIP5 ensemble that are (a) closest and (b) farthest from the reference pattern in Fig. 2. (c and d) Same as Fig. 8a except showing two selected members of the CESM-LE that are (c) closest and (d) farthest from the reference pattern in Fig. 2. (e) PDO time series from all ensemble members; all time series are smoothed with the Zhang et al. filter (used in Fig. 1c). Thin gray lines represent each ensemble member, the thin black solid (dashed) line in the CMIP5 panel represents model A (B), and the thick black line is the ensemble mean for each set of models.

Newman et al. 2016

Observed vs modeled

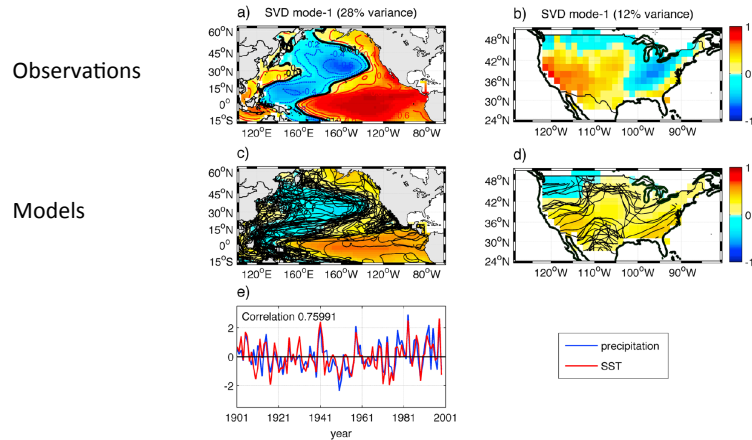


Figure 1. Observed loading patterns of first SVD mode for (a) SST and (b) precipitation, and SVD time series, for (c) winter (in normalized values). Average leading SVD loading patterns for all the models for (Figure 1c) SST and (Figure 1d) precipitation. The SVD loading patterns are expressed as a correlation between SVD time series and respective variables. (e) Red and blue lines denote SST and precipitation, respectively. Black lines in Figures 1c and 1d indicate zero contour lines for individual models.

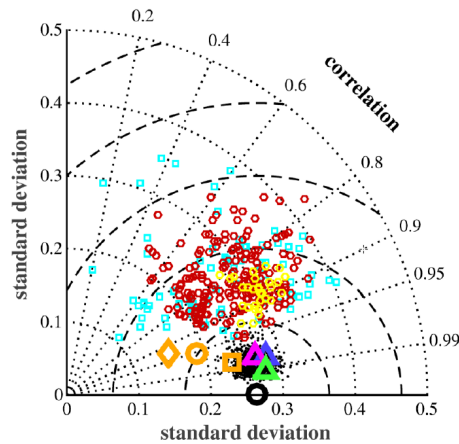


Figure 2. Taylor diagram (Taylor et al. 2001) comparing the reference PDO (HadISST) pattern (Fig. 1a, black circle) with variations due to sampling, observational dataset, and geographical domain; and to PDOs determined from CGCMs run with historical radiative forcing. In this diagram, the distance of a point from the origin is the pattern standard deviation normalized by the reference pattern standard deviation, and the distance from the reference point (at [1,0]) is the root mean square (rms) error normalized by the reference pattern standard deviation, indicated by the dashed semicircles spaced at an interval of 0.5. The pattern correlation, decreasing in a counterclockwise azimuthal direction, is mathematically related to these two quantities. The analysis is taken only over the North Pacific PDO domain (20°N-70°N). Black dots: PDO estimates based on the 50yr Monte Carlo subsamples; triangles: PDO determined from the ERSSTv3b (blue), COBE (green), and Kaplan (magenta) observed data sets; orange symbols: SSTA structure (within the North Pacific PDO region) associated with the leading SSTA EOF, where the southern border of the Pacific domain is instead 0° (square), 20°S (diamond), and 70°S (circle). Also shown are the CMIP3 (cyan), CMIP5 (red), and CESM-LE (yellow) historical simulation PDOs. EOF spatial patterns were interpolated to the 2° by 2° grid used for the reference pattern. Due to differences in landmasks, metrics for the Taylor diagram were calculated over ocean points that were in common between each model and the HadISST data.

Newman et al. 2016

Model skill vs resolution

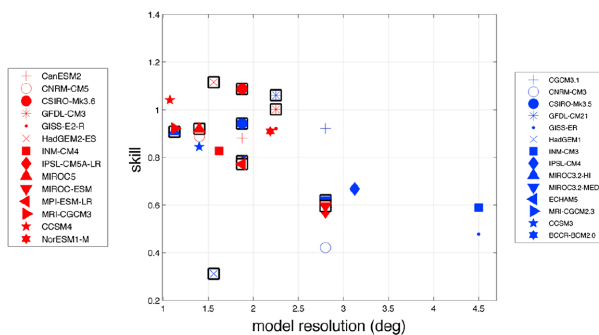


Figure 3. The models' skill with respect to horizontal resolution. Blue and red symbols represent CMIP3 and CMIP5 models, respectively, while black squares indicate the models that did not improve horizontal resolution from CMIP3 to CMIP5. A perfect model would have skill of $\sqrt{2}$.

Polade et al. 2013

Predictability

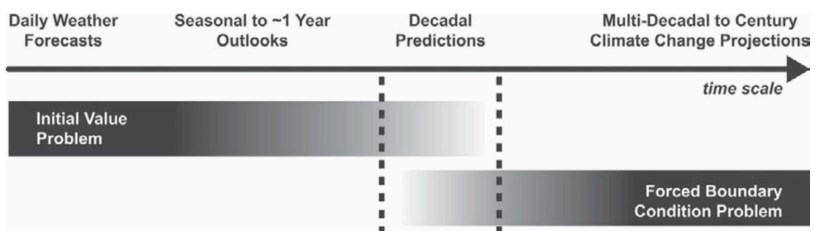
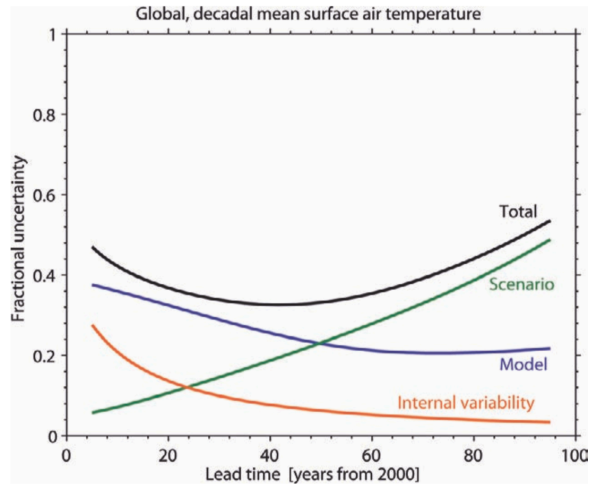


FIG. 2. Schematic illustrating progression from initial value problems with daily weather forecasts at one end, and multidecadal to century projections as a forced boundary condition problem at the other, with seasonal and decadal prediction in between.

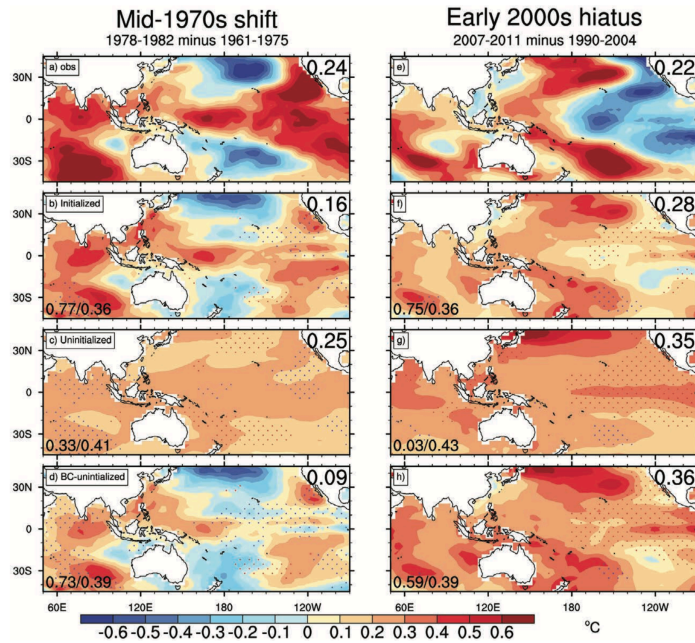
Meehl et al. 2009

Sources of uncertainty



Meehl et al. 2009

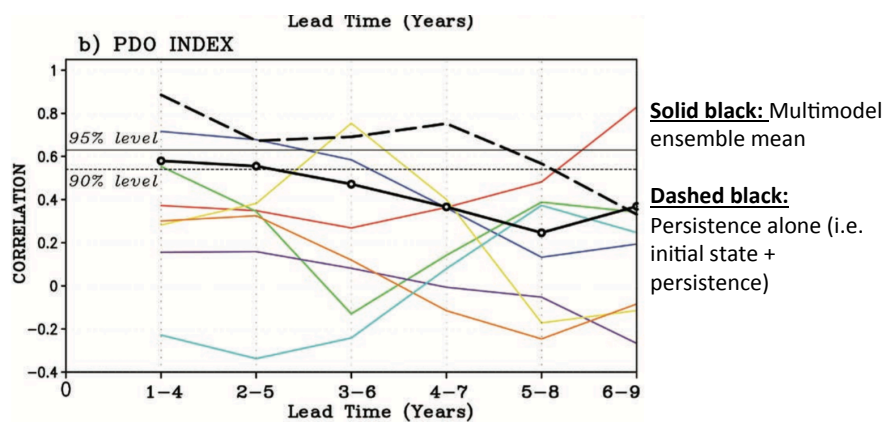
Predictability



Meehl et al. 2014

Predictability

Still limited to a few years in advance

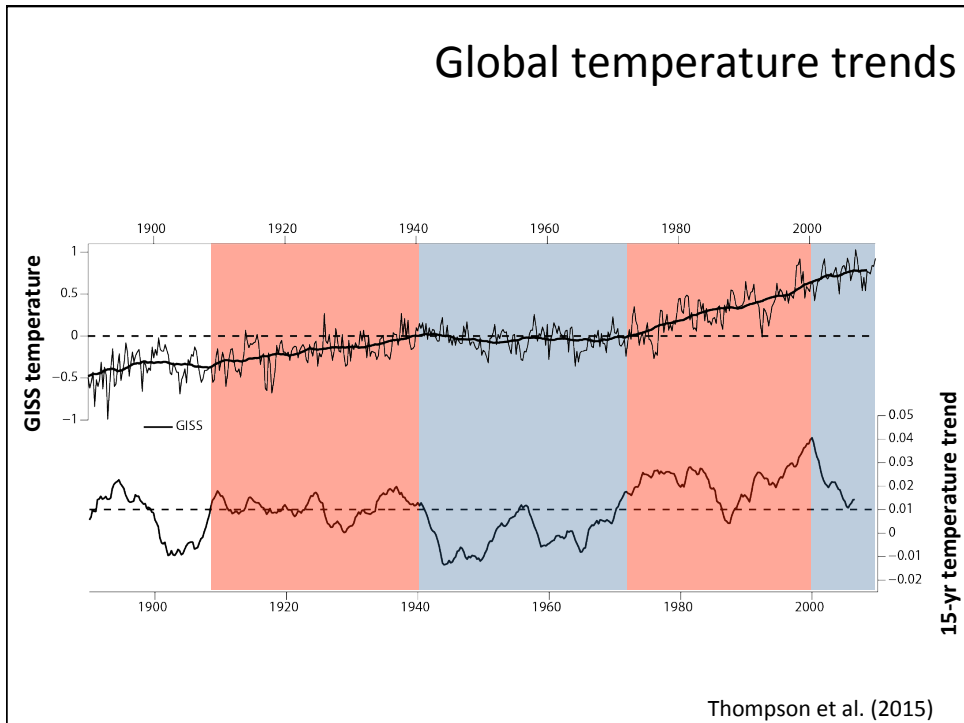
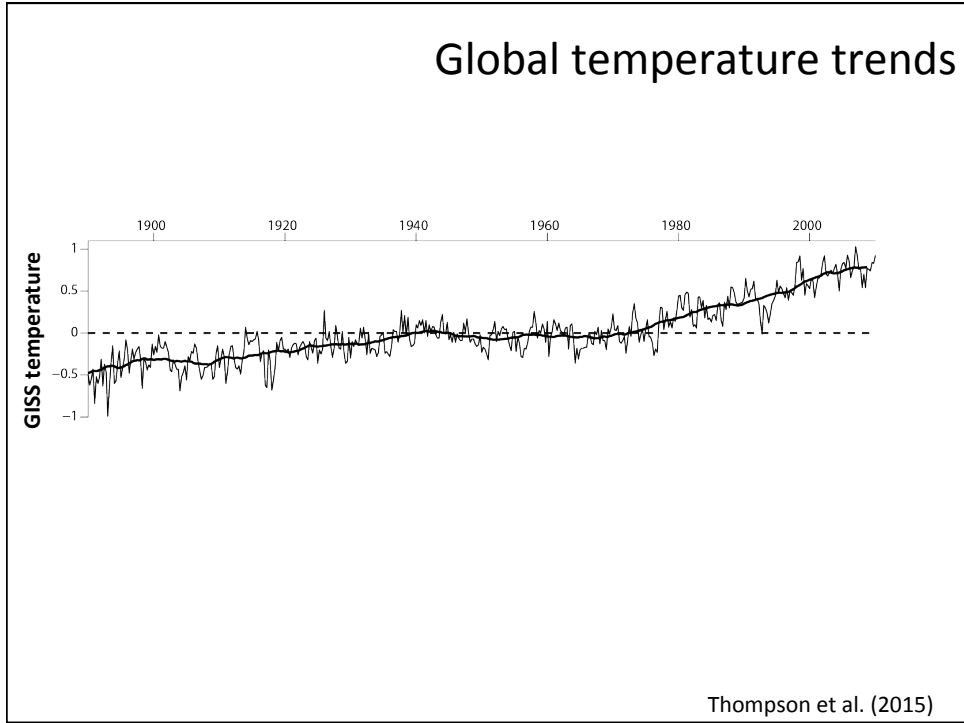


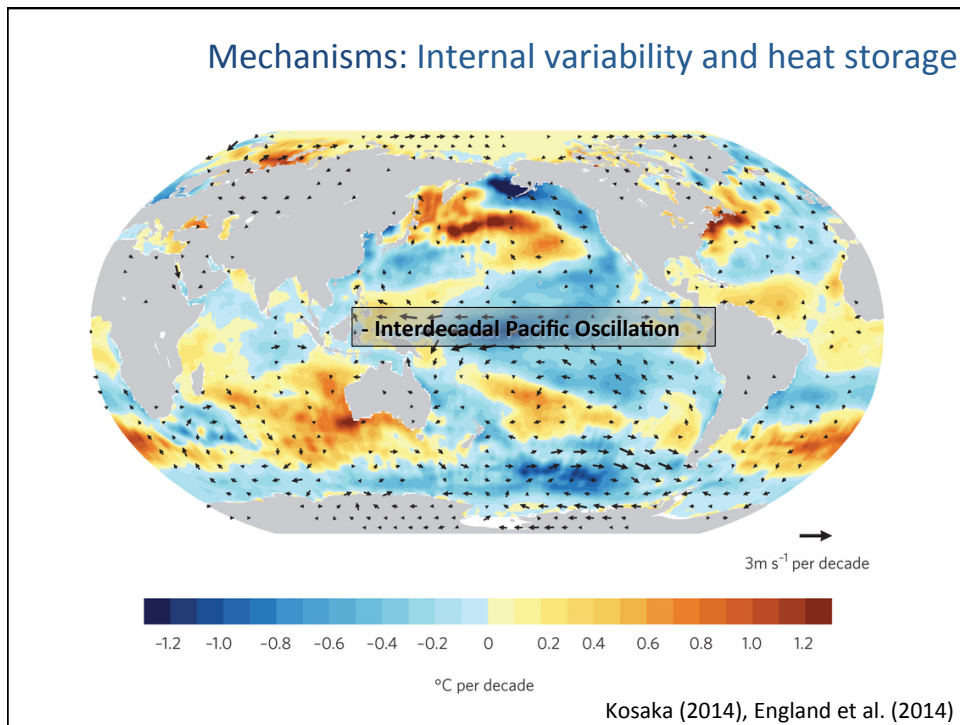
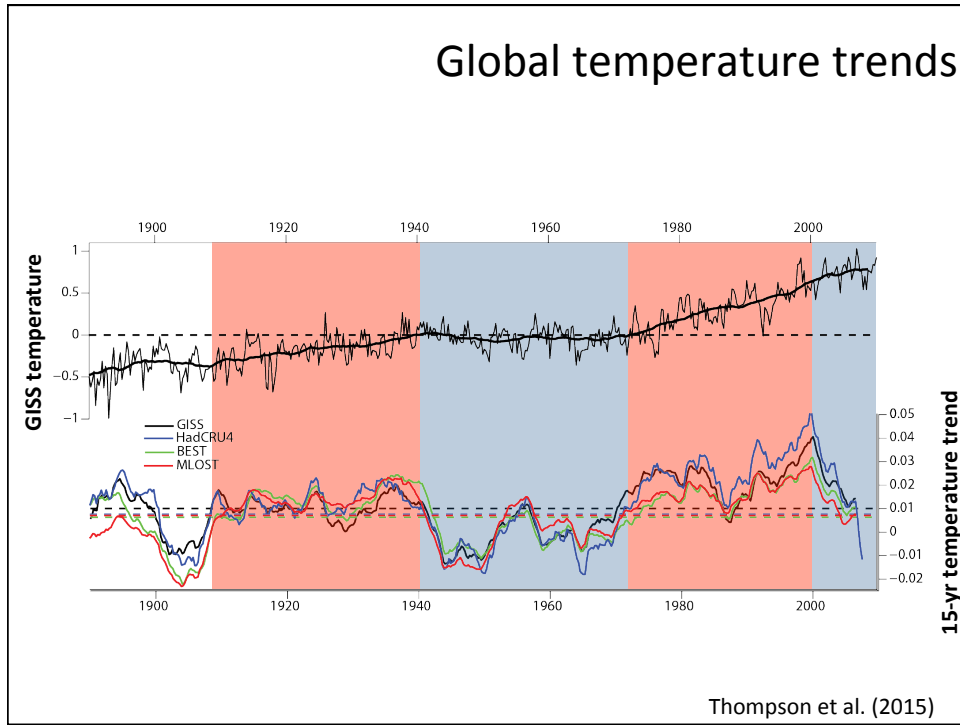
Meehl et al. 2014

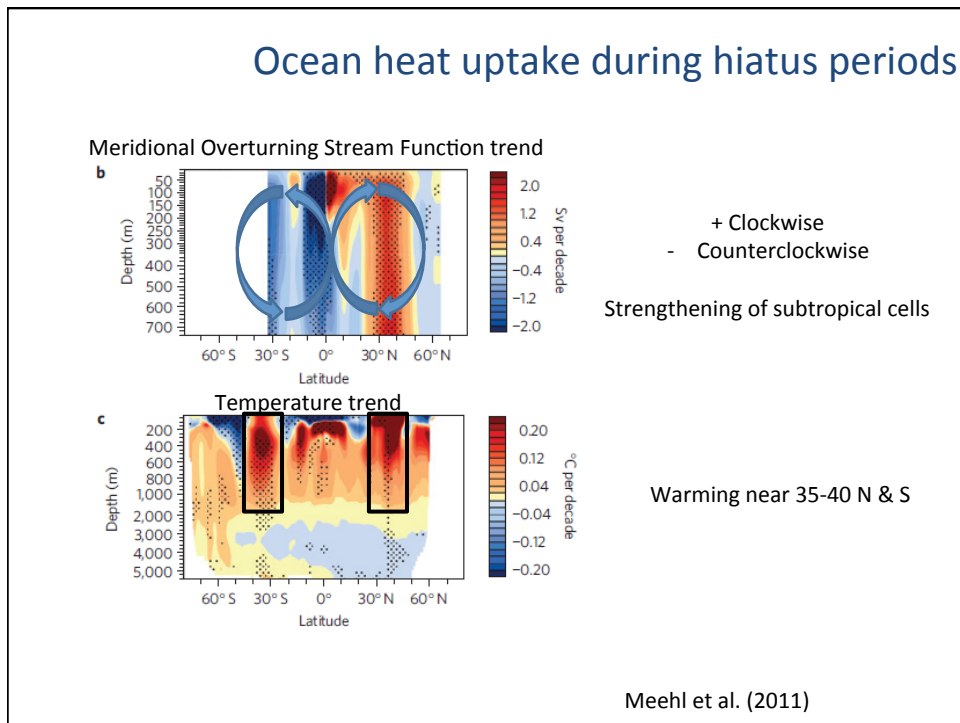
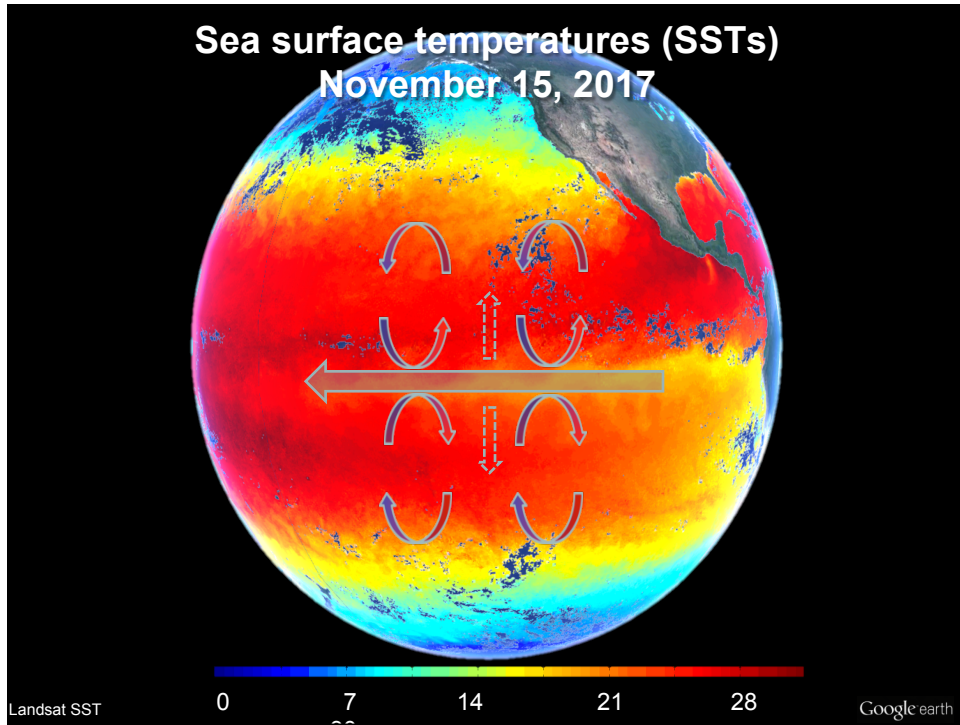
Importance of PDV predictability?

PDV thought to play a role in modulating

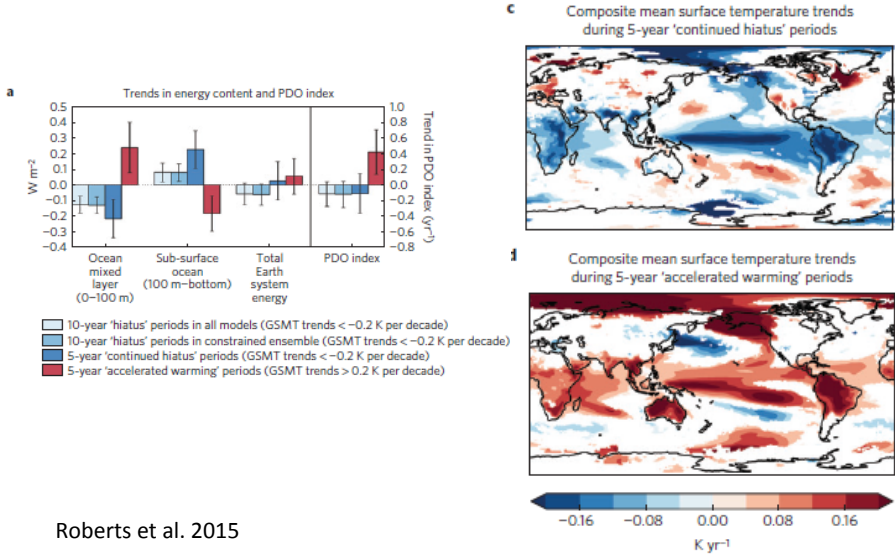
1. ENSO
2. Rate of global warming
3. ...?





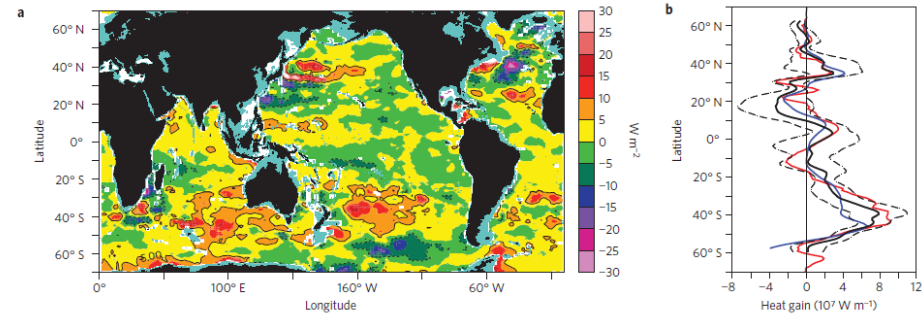


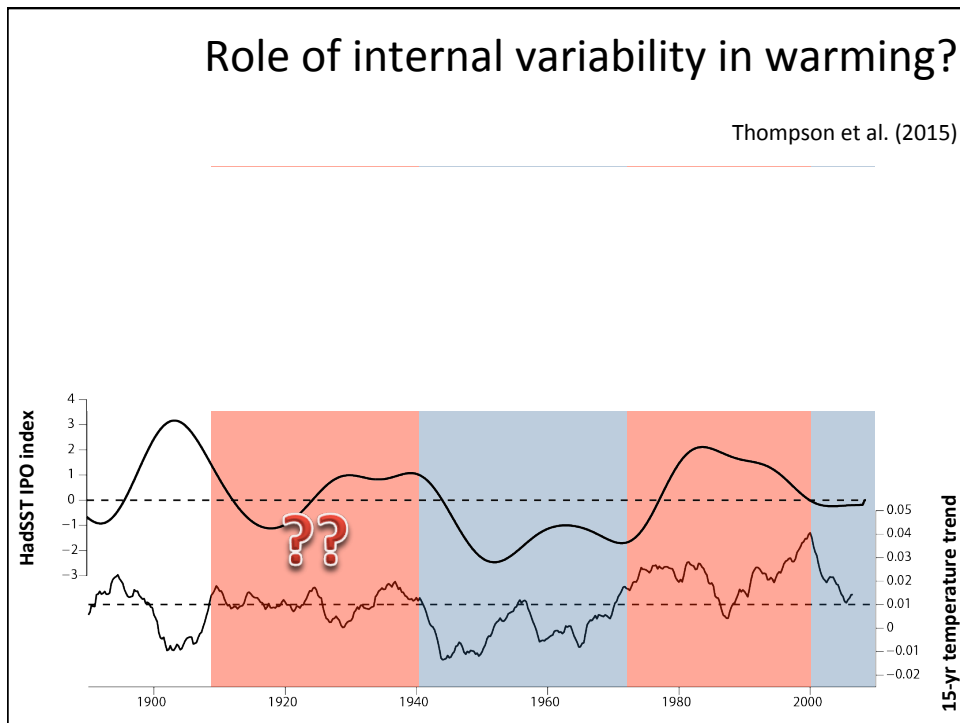
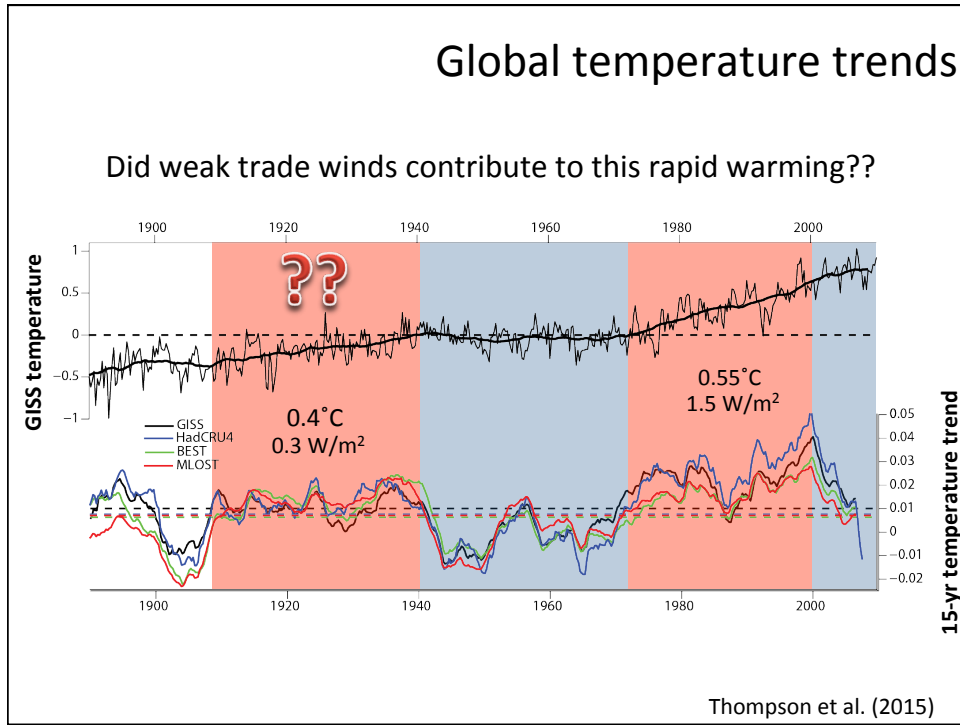
Ocean heat uptake during hiatus periods



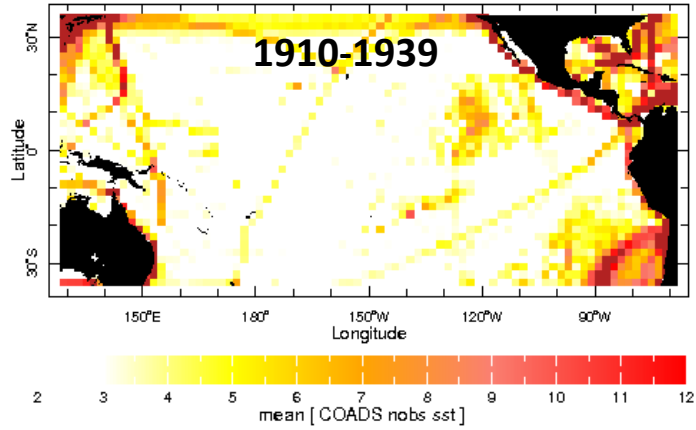
Ocean heat uptake since 2006

Trend in ocean heat content (0-2000m) 2006-2013





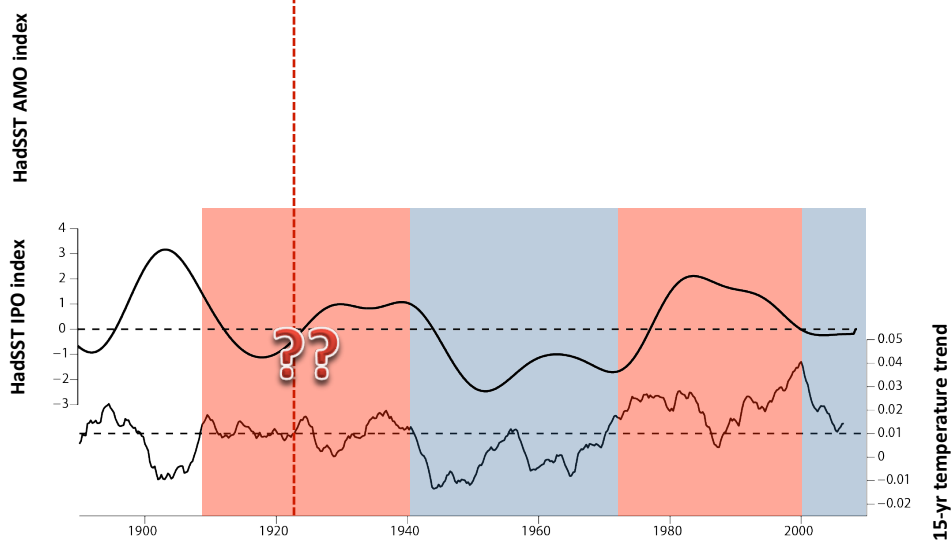
Number of observations per year



Thompson et al. (2015)

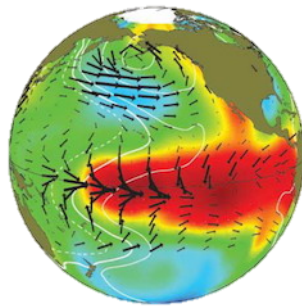
Role of internal variability in warming?

Thompson et al. (2015)



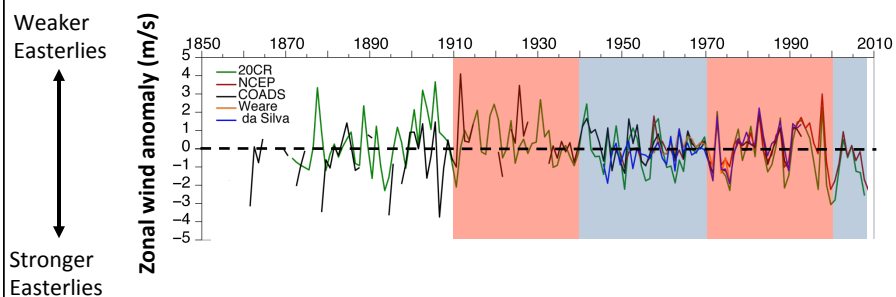
Role of internal variability in warming?

- Early century warming ***too large*** to be driven only by ***external forces*** (CO₂, solar)
- Internal variability key!
 - Atlantic warming: 15 years later
 - Role of Pacific winds?

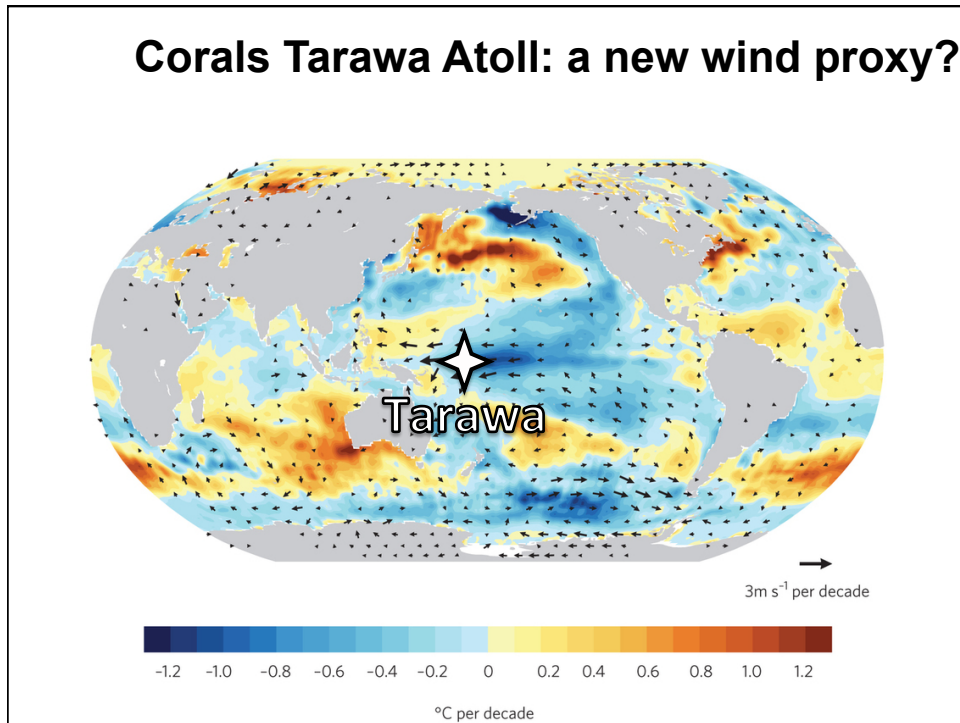
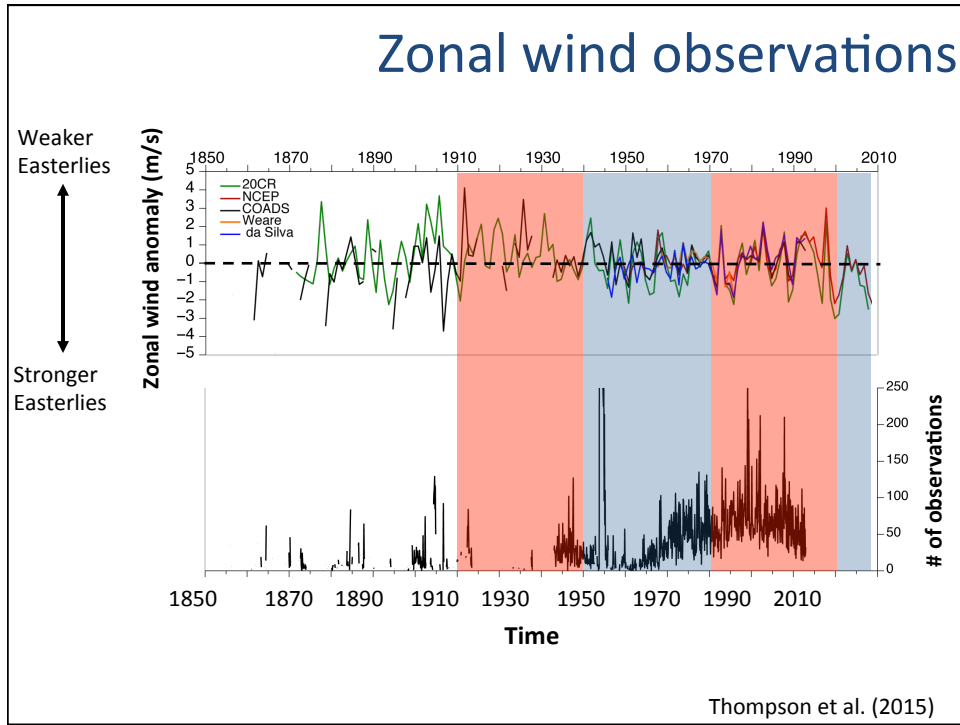


Weak trade winds contribute to this rapid warming??

Zonal wind observations

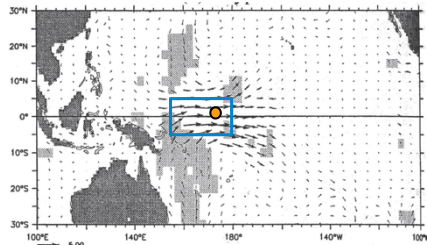


Thompson et al. (2015)



Corals Tarawa Atoll: a new wind proxy?

location

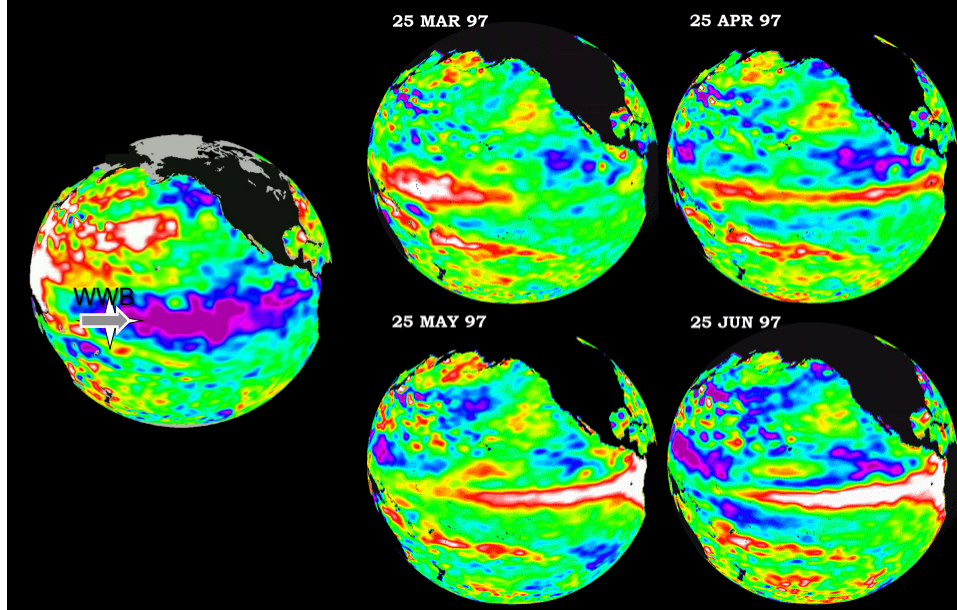


(Lagaine et al., 2004)

Westerly Wind Events/Bursts (WWE):

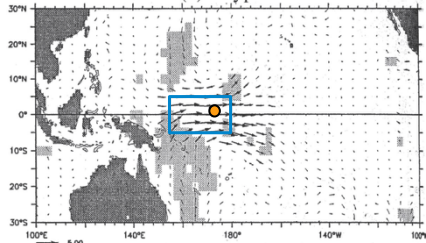
→ strong, short-lived (6-15 days)
westerly wind gusts that occur
before and during El Niño events

Role of westerly winds in ENSO



Corals Tarawa Atoll: a new wind proxy?

location



(Lagaigne et al., 2004)

&

geography



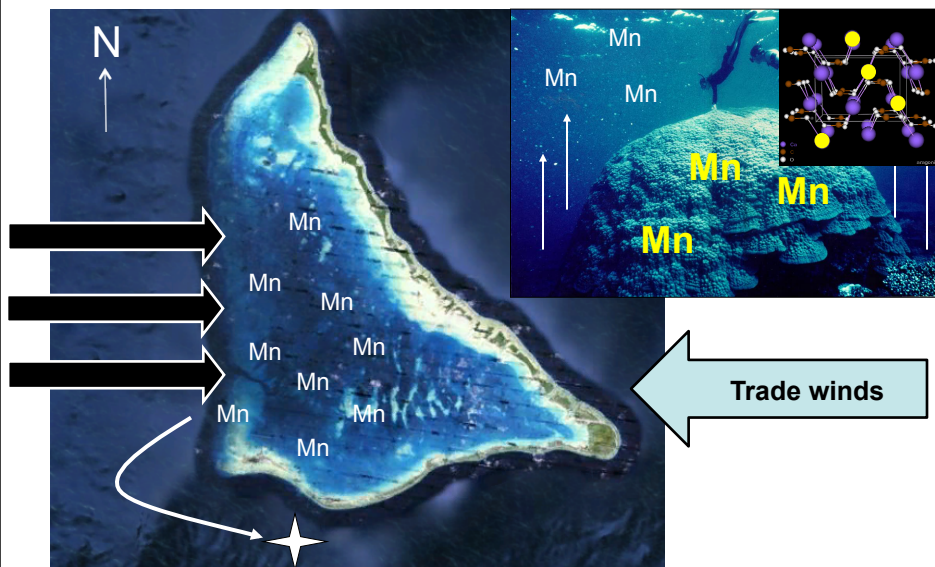
Westerly Wind Events/Bursts (WWE):

→ strong, short-lived (6-15 days) westerly wind gusts that occur before and during El Niño events

Open and westward-facing lagoon

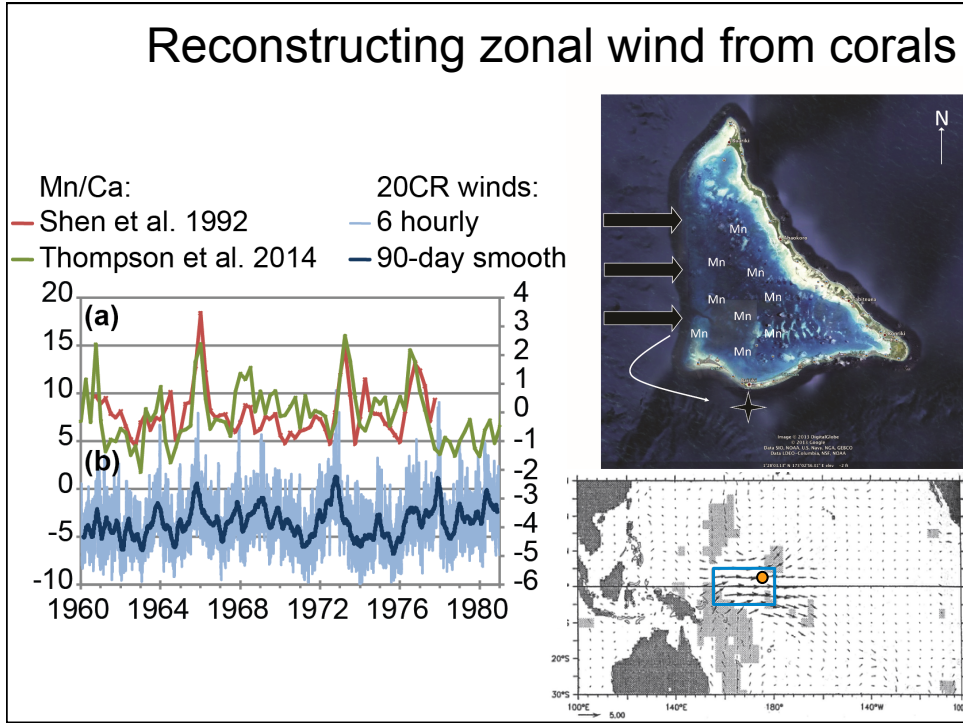
→ sheltered from easterly trade winds, Mn accumulate in lagoon sediments

Reconstructing zonal wind from corals



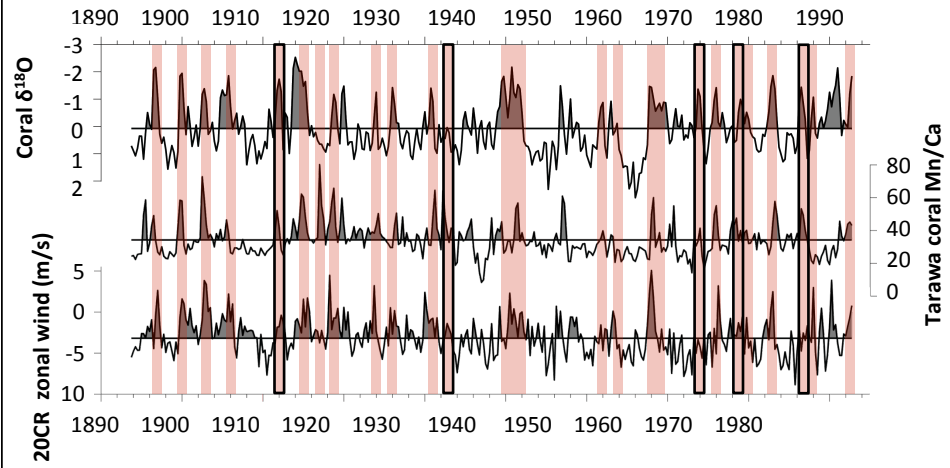
Thompson et al. (2015)

Reconstructing zonal wind from corals



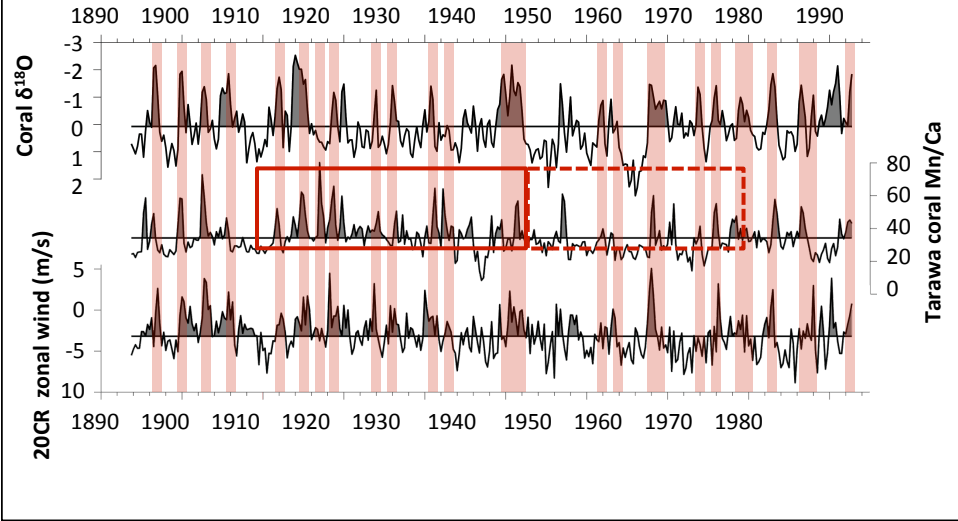
Mn/Ca proof-of-concept: historical El Niños

Thompson et al. (2015)



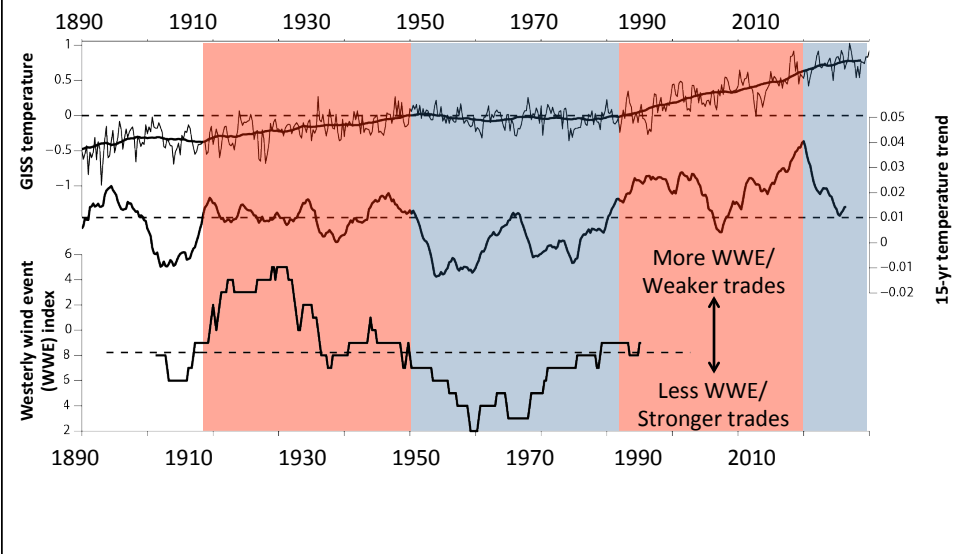
Mn/Ca proof-of-concept: historical El Niños

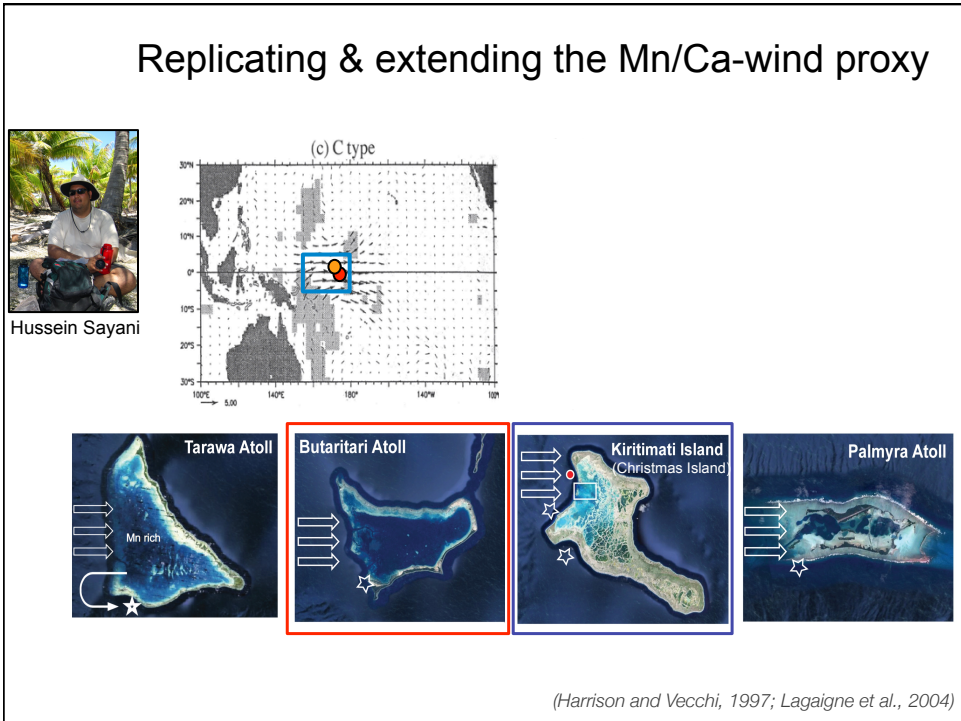
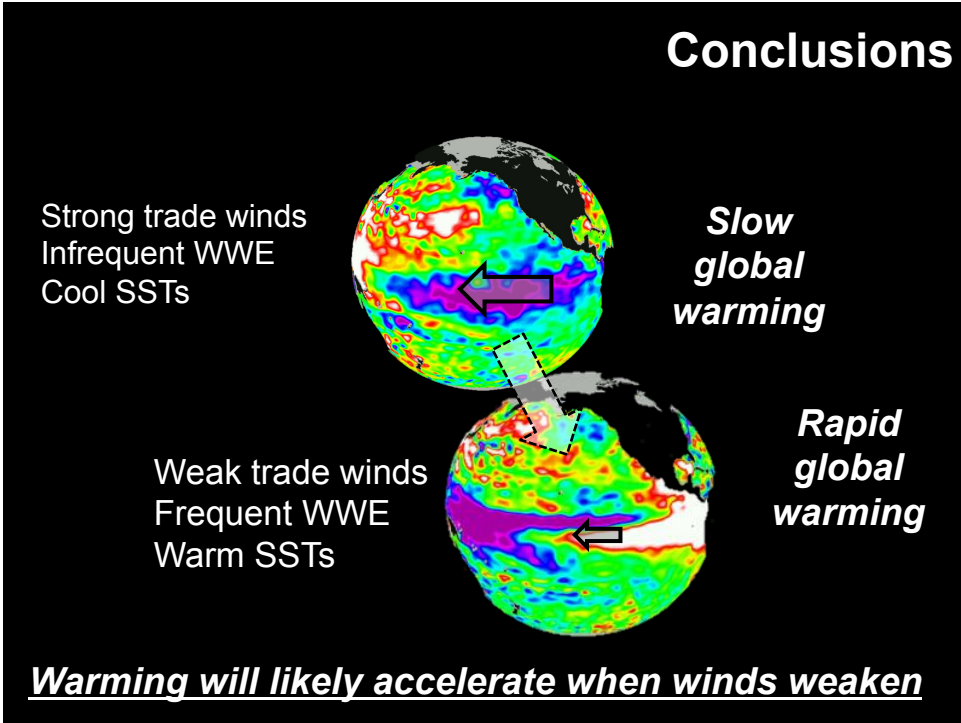
Thompson et al. (2015)

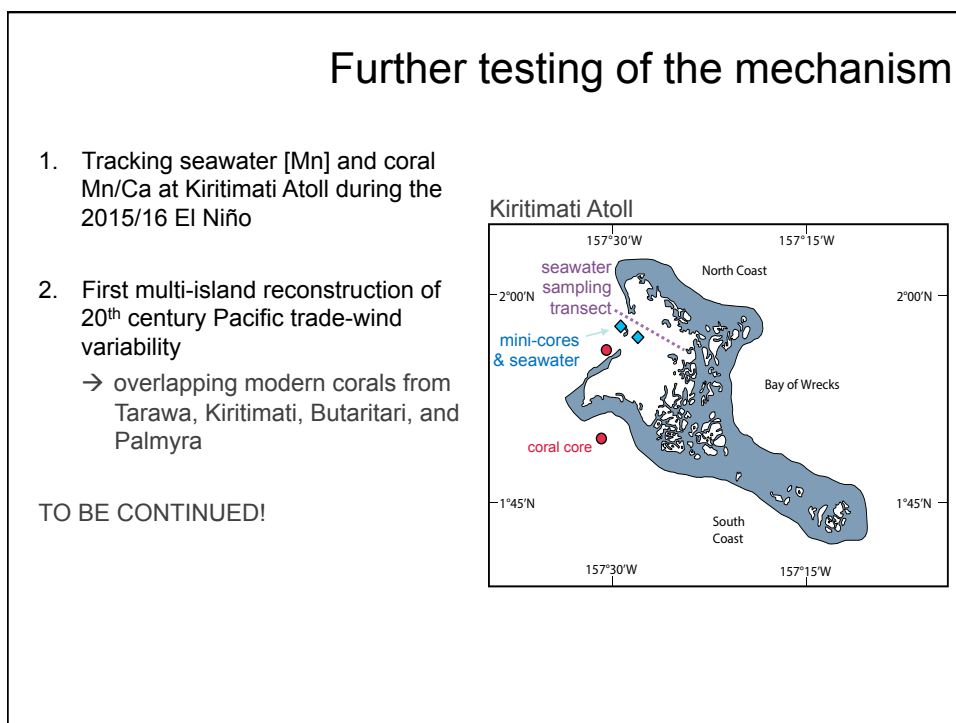
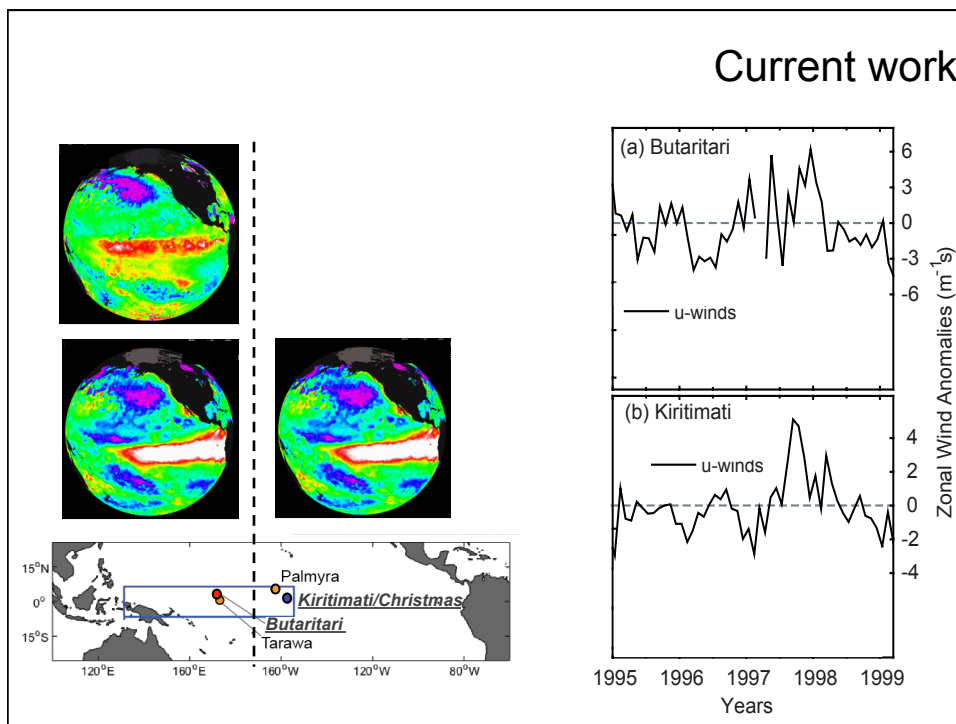


Decadal variability in westerly winds

Thompson et al. (2015)

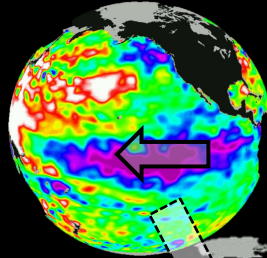






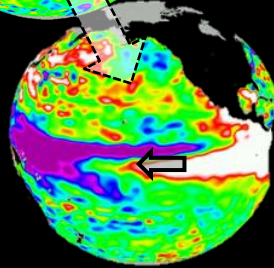
To be continued– what is to come??

Strong trade winds
Infrequent WWE
Cool SSTs



*Slow
global
warming*

Weak trade winds
Frequent WWE
Warm SSTs



*Rapid
global
warming*

Warming will likely accelerate when winds weaken